Volume 1 | Number 1 | Jan 2013 | Pages 1–100

PCCP

Physical Chemistry Chemical Physics
www.rsc.org/pccp

ROYAL SOCIETY OF CHEMISTRY

ROYAL SOCIETY OF CHEMISTRY

www.rsc.org/pccp

Graphical abstract

Radiation-induced color change of [BMIm][NTf$_2$] originates from the formation of double bonds in cations and various associated species containing [BMIm-H$_2$][NTf$_2$].

PCCP

ARTICLE

Towards understanding the color change of 1-butyl-3-methylimidazolium bis(trifluoromethylsulfonyl)imide during gamma irradiation: an experimental and theoretical study†

Shuojue Wang,[a] Junzi Liu,[b] Liyong Yuan,[c] Zhenpeng Cui,[a] Jing Peng,[a] Jiuqiang Li,[a] Maolin Zhai*[a] and Wenjian Liu*[b]

The application of room-temperature ionic liquids (RTILs) in nuclear spent fuel recycling requires a comprehensive knowledge of radiation effects on RTILs. Although preliminary studies indicate relatively high radiation stability of RTILs, little attention is paid to the color change of RTILs, an obvious phenomenon of RTILs during irradiation. In this paper, we have investigated radiation-induced darkening and decoloration of 1-butyl-3-methylimidazolium bis(trifluoromethylsulfonyl)imide ([BMIm][NTf$_2$]), an ionic liquid representing the most popular class of RTILs, by means of UV–Vis analysis and time-dependent density functional theory calculations. Based on the experimental and computational results, it is proposed that the color change of [BMIm][NTf$_2$] upon irradiation originates from the formation of double bonds in the aliphatic chains of pristine organic cations (or radiolysis products of RTILs) and various associated species containing these "double-bond products". This work shines light on the understanding of radiation-induced color change of RTILs.

Introduction

Room-temperature ionic liquids (RTILs) are molten salts with low melting points (< 373 K). In the past few years, RTILs have received considerable attention due to their unique physical and chemical properties including negligible vapor pressure, high thermal stability, nonflammability, wide electrochemical window, and good solubility for a large variety of chemical species.[1, 2] As a result, they are considered as attractive media in nuclear fuel cycle processing for liquid/liquid extraction of actinides, lanthanides and other radioactive nuclides from nuclear waste.[3-5] RTILs can be also used as green solvents or additives for radiation-induced polymerization[6, 7] and radiation preparation of metal nanoparticles.[8, 9]

If RTILs are to be used in nuclear spent fuel recycling or radiation preparation of polymers and nanoparticles, however, they should not undergo significant decomposition when exposed to radiation. Hence, a comprehensive knowledge of radiation effects on RTILs is of primary importance. Allen et al.[10] assessed radiochemical stability of 1,3-dialkylimidazolium-based hydrophilic RTILs and found that less than 1% of the tested RTILs underwent radiolysis after irradiation at 400 kGy, implying high radiation stability of RTILs. Berthon et al.[11] studied hydrophobic RTILs containing 1,3-dialkylimidazolium cation and reported similar results. Moreover, as shown by Moisy et al.[12] in their study on the radiation stability of methyltributyl ammonium bis(trifluoromethylsulfonyl)imide ([N$_{1444}$][NTf$_2$]), [N$_{1444}$][NTf$_2$] with aliphatic cations was stable at high doses. Shkrob et al.[13-18] systematically examined the radiolytic degradation of constituent anions and cations in RTILs by electron paramagnetic resonance spectroscopy and provided some radiation resistant RTILs such as RTILs containing 1-benzylpyridinium

cations or *o*-benzenedisulfonimide anions. We reported,[19, 20] for the first time, the influence of radiation on RTILs for the extraction of metal ions, and found that the extraction efficiencies decreased when irradiated RTILs were used as diluents, which was caused by the competition between radiation-generated H$^+$ and metal ions to interact with extracting agents. The recovery of extraction of metal ions can readily be achieved by washing the irradiated RTILs with water.

All the accumulated results reveal that RTILs are relatively radiation resistant, but one interesting phenomenon is that they exhibit obvious darkening when irradiated[10, 11, 21, 22]. A thorough investigation of radiation-induced color change will help us better understand radiation effects on RTILs. Up to now, very few studies have focused on the decoloration of irradiated RTILs and identification of the colored products. Recently, we preliminarily reported the decoloration of [BMIm][NTf$_2$] after irradiation,[23] where [BMIm]$^+$ is 1-butyl-3-methylimidazolium and [NTf$_2$]$^-$ is bis(trifluoromethylsulfonyl)imide, by incorporating HNO$_3$ or KMnO$_4$ into irradiated [BMIm][NTf$_2$]. However, the understanding of radiation-induced color change of RTILs is still preliminary. One particular obstacle lies in that the "colored products" in irradiated RTILs are of a very small quantity, such that it is difficult to identify or separate them from various radiolysis products. A possible solution to the problem is provided here. By means of UV–Vis analysis and time-dependent density functional theory (TDDFT) calculations, combined with ESI mass spectroscopy, the underlying reason for color change of irradiated [BMIm][NTf$_2$] was elucidated. Additionally, the radiation effects on some other RTILs were investigated using UV–Vis analysis for comparison. Simple ways to decolor the irradiated RTILs were also presented.

Experimental

Materials

1-butyl-3-methylimidazolium hexafluorophosphate ([BMIm][PF$_6$]) and RTILs consisting of [BMIm]$^+$, 1-butyl-1-methylpyrrolidinium ([BMPyrr]$^+$), [N$_{1444}$]$^+$ cations and [NTf$_2$]$^-$ anion were all colorless and obtained from Lanzhou Greenchem ILS, LICP. CAS. China. The purity of all the ILs was more than 99%. The water content was less than 250 ppm for each kind of RTIL, measured by Karl-Fischer titration. The obtained RTILs possessed high optical quality and can be used for spectroscopic studies according to their color and UV-Vis spectra.[24] All other chemicals were analytically pure, and used as received.

Sample irradiation

RTILs were sealed in glass tubes and deaerated by bubbling argon for 30 min before irradiation. The samples were then subjected to γ-irradiation with a dose of 50–400 kGy (dose rate: 130–145 Gy min^{-1}) at room temperature in a ^{60}Co source at Department of Applied Chemistry of Peking University. The absorbed dose was monitored using a conventional ferrous sulfate dosimeter.

Decoloration treatment of irradiated RTILs

To decolor the irradiated RTILs, HNO$_3$ oxidation and O$_3$ treatment were employed. The HNO$_3$ oxidation was performed according to the procedure previously reported.[23] As to O$_3$ treatment, the irradiated samples were purged with ozone gas for 30 min.

Sample analysis

The ATR-IR measurements were carried out with a Nicolet (NICOLET iN10MX) spectrometer. ^{1}H NMR spectra of the samples in deuterated DMSO were measured using Bruker AVANCE III 500 MHz NMR spectrometer. The UV–Vis absorbance was recorded on a UV-3010 spectrophotometer (Hitachi) with a cuvette of 1 cm path length, and the samples were diluted with acetonitrile before measurements in different ratios. ESI-MS spectra were acquired in positive ionization mode using a Bruker APEX IV Fourier Transform Ion Cyclotron Resonance Mass Spectrometer. Samples were diluted in pure methanol solutions.

Geometry optimization and excited state calculations

The geometries of imidazolium cations were optimized by using the B3LYP density functional and the 6-31G(d,p) basis set. All optimized geometries were confirmed by frequency calculation with no imaginary frequencies. Subsequent TDDFT calculations of the excited states employed the same functional but the 6-311G(d,p) basis set. All calculations were performed with Gaussian 09 program package.[25]

Results and discussion

Radiation-induced color change

ATR-IR and ^{1}H NMR spectra of the studied RTILs before and after irradiation reveal that no significant degradation occurred (Fig. S1 and S2, ESI†). Although RTILs had relatively high radiation stability, they exhibited obvious darkening after γ-irradiation, which was similar to other reports.[11, 22] The darkening was more intense with the increase of absorbed dose (inset of Fig. 1). In the studied dose range, no precipitate was found. In order to further analyze the radiation-induced darkening of RTILs, the UV–Vis spectra of diluted samples were measured using acetonitrile as solvent. According to As shown in Fig. 1, an increase in light absorbance of [BMIm][NTf$_2$] in a wide wavelength range and a distinct absorption

peak at 290 nm occurred after γ-irradiation. Similar observation was reported.[23, 26] While almost no absorption was observed at 290 nm for un-irradiated [BMIm][NTf$_2$] in 300-times dilute acetonitrile solution, an absorbance of ca. 0.57 was obtained after irradiation at 400 kGy, indicating the formation of radiolysis species that have a strong absorption. As [BMIm][NTf$_2$] we used was pure enough, the color and UV absorption originated from the radiolysis of [BMIm][NTf$_2$]. In addition, it should be mentioned that the UV absorption at 200–240 nm was so strong that the "spikes" were inevitable in the spectrum. The "spike area" was displayed just to show strong absorption within the wavelength range.
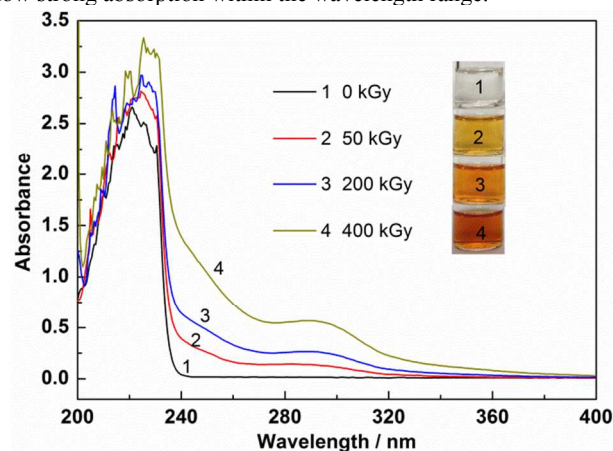

Fig. 1 UV–Vis absorbance spectra of [BMIm][NTf$_2$] before and after irradiation at different doses (dilution factor 300). Inset shows the color of irradiated [BMIm][NTf$_2$] at different doses.

To further probe what leads to the color change and enhanced UV absorption, comparative tests were carried out using a series of RTILs. Fig. 2a shows the UV–Vis spectra and color of irradiated samples containing the same [NTf$_2$]$^-$ anions associated with [BMPyrr]$^+$ and [N$_{1444}$]$^+$ cations. After irradiation, the color darkening and enhanced spectral absorption also occurred in both [BMPyrr][NTf$_2$] and [N$_{1444}$][NTf$_2$]. The two RTILs displayed similar UV-Vis spectra. Different from [BMIm][NTf$_2$] irradiated at the same dose, irradiated [BMPyrr][NTf$_2$] and [N$_{1444}$][NTf$_2$] were yellow in color and the wavelengths of the new distinct absorption peaks were both at 320 nm, suggesting radiolysis products that are different from those of irradiated [BMIm][NTf$_2$]. Since both [BMPyrr][NTf$_2$] and [N$_{1444}$][NTf$_2$] belong to ammonium RTILs, the similar color and similar UV-Vis spectra after irradiation are likely to originate from the radiolysis of ammonium cations. Furthermore, the intensity of broad absorption band at the wavelength ranging from 200 to 400 nm was much weaker for ammonium RTILs ([BMPyrr][NTf$_2$] and [N$_{1444}$][NTf$_2$]) than for aromatic RTIL ([BMIm][NTf$_2$]) following irradiation (note that the dilution factor of [BMIm][NTf$_2$] was twice more than that of [BMPyrr][NTf$_2$] and [N$_{1444}$][NTf$_2$]). This is another evidence to support our supposition that the color darkening and increased UV absorption are related to the radiolysis of cations in RTILs.

The effects of anions on the darkening of RTILs after irradiation were also studied. The UV–Vis spectra of [BMIm][NTf$_2$] and [BMIm][PF$_6$] before and after irradiation at 400 kGy are displayed in Fig. 2b. Compared to [BMIm][NTf$_2$], [BMIm][PF$_6$] prior to and after irradiation showed similar UV-Vis spectra except that the light absorbance of [BMIm][PF$_6$] was stronger than that of [BMIm][NTf$_2$]. After irradiation, the position of the new absorption band in the UV-Vis spectrum of [BMIm][PF$_6$] was also at ~290 nm, implying the formation of radiolysis products from [BMIm]$^+$ with similar structure. [BMIm][PF$_6$] has larger proportion of [BMIm]$^+$

2 | *Phys. Chem. Chem. Phys.*, 2014, **00**, 1-6

This journal is © The Royal Society of Chemistry 2014

than [BMIm][NTf$_2$]. Thus more radiation energy is distributed on the cations of [BMIm][PF$_6$], which leads to the more significant radiation-induced darkening and stronger light absorbance of irradiated [BMIm][PF$_6$].
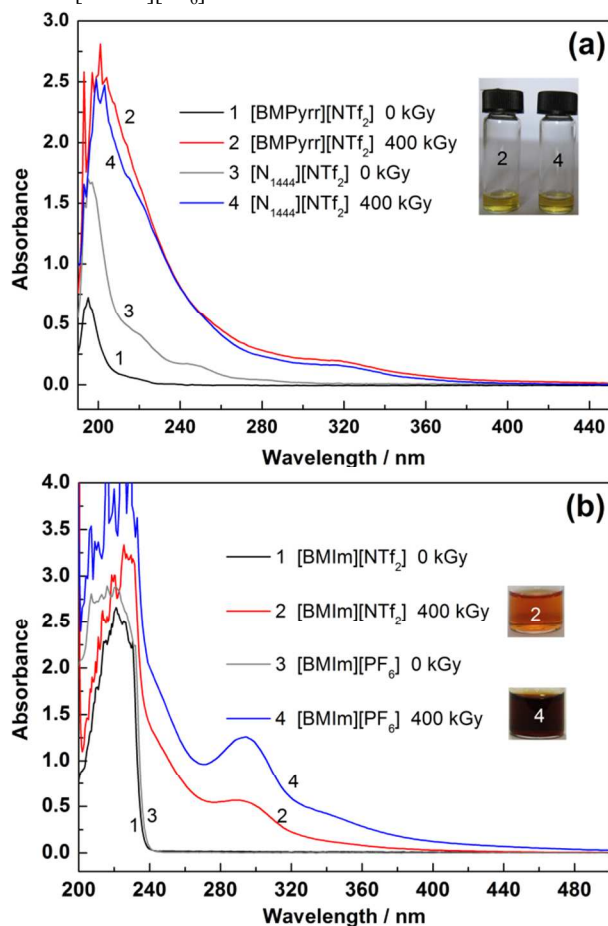

Fig. 2 (a) UV–Vis spectra of [BMPyrr][NTf$_2$] and [N$_{1444}$][NTf$_2$] before and after irradiation at 400 kGy under argon atmosphere (dilution factor 100). (b) UV–Vis spectra of [BMIm][NTf$_2$] and [BMIm][PF$_6$] before and after irradiation at 400 kGy under argon atmosphere (dilution factor 300). Inset of each figure shows the color of corresponding samples. The RTIL samples are all colorless before irradiation, and their pictures are omitted.

Decoloration of irradiated RTILs

Research into decoloration of irradiated RTILs helps to figure out the "colored species". Up to now only the decoloration of irradiated [BMIm][NTf$_2$] by HNO$_3$ or KMnO$_4$ treatment has been reported.[23] Given some problems such as heavy metal pollutions and difficulties in recycling the RTILs following KMnO$_4$ treatment, HNO$_3$ oxidation was carried out. If RTILs are to be used in nuclear spent fuel recycling, they will contact with HNO$_3$ during the extraction stage.[27] Study on decoloration of irradiated RTILs with HNO$_3$ treatment will be helpful in understanding the influence of HNO$_3$ on RTILs. It was found that decoloration of both irradiated [BMIm][NTf$_2$] (a representative of aromatic RTILs) and [BMPyrr][NTf$_2$] (a representative of aliphatic RTILs) can be achieved after HNO$_3$ treatment, accompanied by decreased UV absorption band (Fig. S3, ESI†). Additionally, no obvious change in ^{1}H NMR spectra before and after HNO$_3$ treatment was detected (Fig. S4, ESI†), indicating that HNO$_3$ has almost no impact on the structure of pristine RTILs. Because the "colored products" are in a very small quantity, NMR spectroscopy is unable to identify them.

Considering that the colored radiolysis products can be oxidized, we introduced another oxidizing agent—ozone, by bubbling gas into the irradiated RTILs. Fig. 3a shows effect of O$_3$ on the color and UV–Vis absorption spectra of irradiated [BMIm][NTf$_2$]. As expected, ozone treatment led to a decline of absorbance in a wide wavelength range, as well as the disappearance of absorption peak at 290 nm. Light-colored RTILs were obtained after ozone oxidation. Accordingly, ozone treatment is a much simpler way to achieve the decoloration of RTILs following irradiation, compared with KMnO$_4$ and HNO$_3$ oxidation. [BMPyrr][NTf$_2$] was further investigated for decoloration. It was found that O$_3$ treatment can also decolor irradiated [BMPyrr][NTf$_2$] (Fig. 3b). Consequently HNO$_3$ and O$_3$ oxidation are both common and effective ways to decolor irradiated RTILs. But it is noteworthy that after O$_3$ treatment for decoloration, some small peaks (~10% conversion) were observed in the ^{1}H NMR spectrum. It was difficult to identify the attribution of these peaks. Further study revealed that these peaks originate from slight destruction of [BMIm][NTf$_2$] itself rather than destruction of radiolysis products during O$_3$ oxidation (Fig. S4, ESI†). This indicates that O$_3$ reacts with pristine RTILs and thus O$_3$ oxidation is not an ideal method to decolor irradiated RTILs compared with HNO$_3$ treatment.
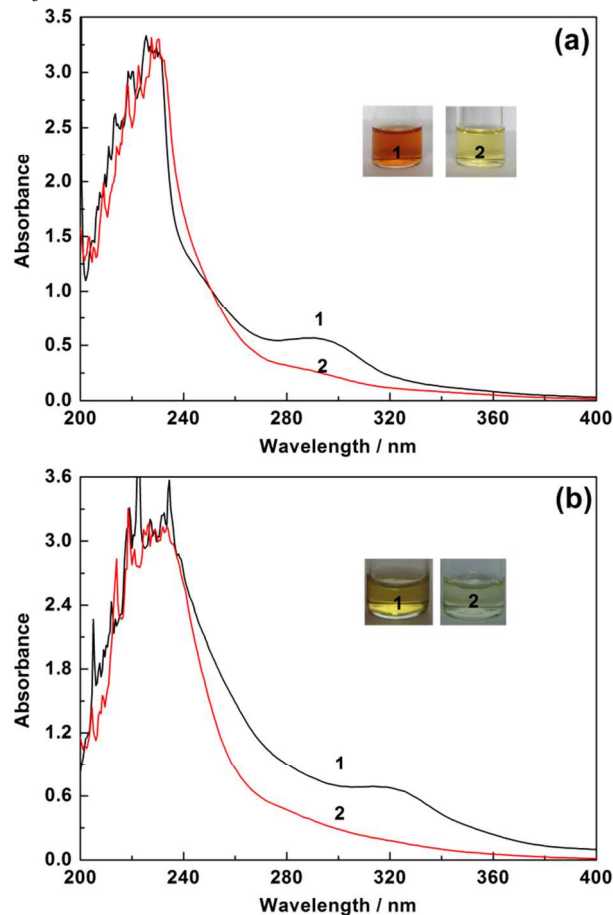

Fig. 3 (a) UV–Vis spectra of irradiated [BMIm][NTf$_2$] with a dilution factor of 300 before (1) and after (2) ozone treatment for 30 min. (b) UV–Vis spectra of irradiated [BMPyrr][NTf$_2$] with a dilution factor of 25 before (1) and after (2) ozone treatment for 30 min. Inset of each figure shows the corresponding color change.

Understanding the color change upon irradiation

We now attempt to identify the "colored species" related to strong light absorption. The investigation of imidazolium-based RTILs

This journal is © The Royal Society of Chemistry 2014

Phys. Chem. Chem. Phys., 2014, **00**, 1-6 | **3**

suggested that the color change may be attributed to oligomerization of imidazolium or imidazole units.[11] During reduction process, a dimer of imidazolium cations can be obtained[28] and the formation of oligomers in irradiated RTILs has been confirmed by NMR and mass spectra.[14] However, aromatic oligomers are generally deemed to be stable on HNO_3, implying that the formation of aromatic oligomers is not a reasonable explanation for the radiation-induced darkening.

The formation of carbenes was also supposed to be responsible for the radiation-induced darkening.[10, 23] Though there are several exceptions, carbenes are generally considered to be reactive and short-lived molecules. To the best of our knowledge, formation of stable carbenes from ammonium and pyrrolidinium is impossible. Although imidazole-2-ylidenes belong to a class of well-known stable carbenes,[29-31] 1,3-dimethyl-imidazol-2-ylidene with a similar structure can be stored in tetrahydrofuran for only several days at low temperature (-30 °C) without substantial decomposition.[30] However the color of irradiated RTILs was maintained, indicating high stability of colored species. Accordingly, it is inferred that the radiation-induced darkening is not attributed to carbenes.

It comes to our notice that the colored species can be oxidized by HNO_3 and O_3. This gives us a hint that the darkening of irradiated RTILs may be assigned to the formation of double bonds in the pristine organic cations or radiolysis products of RTILs. Such radiolysis products are known to be stable at room temperature, in line with the color maintenance of irradiated RTILs observed here. C-centered radicals in the aliphatic chains have been observed in both aliphatic[32] and aromatic RTILs[14, 16] after irradiation. Further hydrogen abstraction from this kind of radicals[33] or disproportionation of these radicals[14] can lead to the degradation products with double bonds in the aliphatic chains of cations. Such radiolysis products were reported in irradiated $[BMIm][NTf_2]^{33}$ and $[N_{1444}][NTf_2]$.[12]

Table 1. $[BMIm][NTf_2]$ samples and corresponding I_{556}/I_{558} ratios [a]

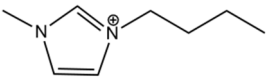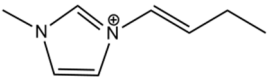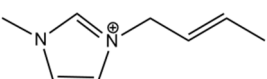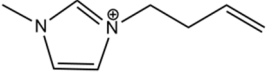| Sample	I_{556}/I_{558} ($\times 10^{-3}$)
Neat $[BMIm][NTf_2]$	ND^b
Irradiated $[BMIm][NTf_2]$	3.765 ± 0.172
Irradiated $[BMIm][NTf_2]$ after HNO_3 treatment	2.671 ± 0.106
Irradiated $[BMIm][NTf_2]$ after O_3 treatment	1.773 ± 0.029

[a] I_{556}/I_{558} refers to the intensity ratio of the peak at $m/z = 556$ and 558, which was obtained from ESI-MS measurement. Each sample has been measured three times under the same condition.
[b] not detected.

Herein the existence of these "double-bond products" in the samples irradiated at 400 kGy and their decrease after decoloration were confirmed by ESI-MS analysis (Table 1 and Fig. S5, ESI†). The peak at $m/z = 558$ observed in the spectrum of un-irradiated $[BMIm][NTf_2]$ is attributed to $[BMIm][NTf_2]$ associated with $[BMIm]^+$. The intensity of this peak is thought to be unchanged after HNO_3 treatment because the radiolytic products of $[BMIm][NTf_2]$ are in a very low yield and HNO_3 has almost no influence on the structure of $[BMIm][NTf_2]$ itself. A signal at $m/z = 556$ was observed in the ESI-MS spectrum of irradiated $[BMIm][NTf_2]$, arising from $[(BMIm)_2NTf_2]^+$. H_2 loss peaks routinely occur in mass spectrometry and therefore only the observation of H_2 loss peak is not a conclusive evidence to support the formation of $[(BMIm)_2NTf_2]^+$ in $[BMIm][NTf_2]$ after irradiation. However, the appearance of the signal at $m/z = 556$ in the spectrum of irradiated sample and the reduced I_{556}/I_{558} ratio for the irradiated $[BMIm][NTf_2]$ after HNO_3 or O_3 oxidation indicate the existence of $[(BMIm)_2NTf_2]^+$ in irradiated $[BMIm][NTf_2]$. Based on the structure of the cation, two kinds of $[(BMIm)_2(NTf_2)]^+$ are involved: a dimer of two primary cation radicals ($[(BMIm)_2]^{2+}$) associated with $[NTf_2]^-$

or $[Bu(-H_2)MeIm]^+$ associated with $[BMIm][NTf_2]$. As the dimer $[(BMIm)_2]^{2+}$ is considered to be stable on HNO_3, the decline of I_{556}/I_{558} value after decoloration (Table 1) indicates that the latter one is responsible for the appearance of the peak. As O_3 destroys the structure of $[BMIm][NTf_2]$ to some degree, after O_3 treatment the signal at $m/z = 558$ will decreased. Consequently the I_{556}/I_{558} value will be larger on the supposition that the intensity of the peak at $m/z = 556$ is maintained. Herein the reduced I_{556}/I_{558} value during O_3 treatment implies the declined signal at $m/z = 556$. The signal ascribed to formation of double bonds was also observed in the ESI-MS spectrum of irradiated $[BMPyrr][NTf_2]$ (Fig. S5, ESI†).

Table 2. Calculated UV-Vis spectra of immidazolium cations

Abbreviation	Absorption peak (nm)	oscillator strength
$[BMIm]^+$	198	0.076
	188	0.010
	187	0.082
	181	0.008
	170	0.125
	165	0.003
	164	0.050
	162	0.023
	158	0.042
	157	0.028
$[BMIm-H_2]^+$-1	243	0.360
	216	0.050
	201	0.095
	189	0.001
	184	0.002
	177	0.108
	172	0.267
	168	0.010
	165	0.028
	162	0.004
$[BMIm-H_2]^+$-2	245	0.001
	203	0.002
	197	0.101
	177	0.050
	175	0.564
	171	0.077
	167	0.004
	164	0.021
	159	0.049
	157	0.234
$[BMIm-H_2]^+$-3	263	0.029
	220	0.005
	197	0.086
	181	0.008
	180	0.042
	174	0.001
	171	0.102
	168	0.134
	166	0.326
	164	0.031

Since imidazolium RTILs are the most popular RTILs and have been widely investigated as attractive solvents in nuclear fuel cycle, the following discussion is concentrated on $[BMIm][NTf_2]$. To the best of our knowledge, no literature has reported UV-Vis data of RTILs containing similar cation structure to that as supposed. As concluded above, the colored species originate in the radiolysis of cations in RTILs. We calculated the excitation energies of the lowest 10 excited states for $[BMIm]^+$ and $[BMIm-H_2]^+$ using TDDFT. For simplification, a single imidazolium cation was calculated without considering the influence of solvation and anions. Given the complexity of irradiated RTILs, the calculated UV-Vis spectrum of

4 | *Phys. Chem. Chem. Phys.*, 2014, **00**, 1-6

This journal is © The Royal Society of Chemistry 2014

[BMIm]$^+$ (Table 2) was consistent with the trend of experimental data (Fig. 1). The calculated absorption peaks ranging from 198 nm to 157 nm (Table 2) accorded with the UV absorption band at 240–200 nm in the UV-Vis spectrum of neat [BMIm][NTf$_2$] (Fig. 1) with about 40 nm blue shift. The wavelength discrepancies between calculated and experimental results are to a large extent due to neglect of effects of solvation and ionic pair. The calculated results of optimized structure of [BMIm-H$_2$]$^+$-1 showed absorption peaks at 216 nm and 201 nm together with an absorption peak at 243 nm possessing strong oscillator strength (Table 2), which explains the broad absorption band at 300–200 nm accompanied by the distinct peak at 290 nm in the UV-Vis spectrum of irradiated [BMIm][NTf$_2$] (Fig. 1). The peaks with great oscillator strength at 177 nm and 172 nm of [BMIm-H$_2$]$^+$-1 were in accordance with the stronger absorption band at 240–200 nm in the UV-Vis spectrum of [BMIm][NTf$_2$] after irradiation in Fig. 1. The calculated UV-Vis spectra of [BMIm-H$_2$]$^+$ with different double bond positions were similar to that of [BMIm-H$_2$]$^+$-1. It is noteworthy that the spectrum of irradiated [BMIm][NTf$_2$] is a combined result of [BMIm][NTf$_2$] molecules that have not undergone radiolysis (in a majority) and other "colored products" (in a small quantity).
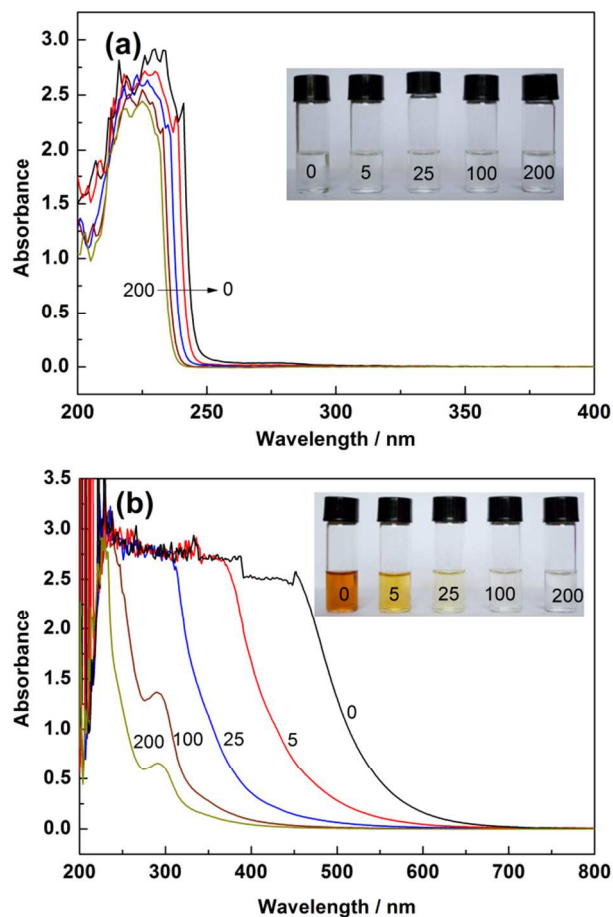

Fig. 4 UV-Vis spectra of [BMIm][NTf] at different dilution factors before (a) and after (b) irradiation at 400 kGy. Inset of each figure shows the corresponding color of different samples. The numbers indicate the corresponding dilution factors.

The above results and discussion reveal that the formation of double bonds on the aliphatic chains is likely to be responsible for the color darkening and strong light absorption in irradiated [BMIm][NTf$_2$]. However, there is still a problem that needs to be solved: why did irradiated [BMIm][NTf$_2$], whose UV-Vis spectrum

displayed almost no absorption above 400 nm, turn orange? To understand this phenomenon, [BMIm][NTf$_2$] was diluted with acetonitrile in different ratios. The UV-Vis spectra and color of [BMIm][NTf$_2$] at different dilution factors are displayed in Fig. 4. The UV-Vis spectra of un-irradiated [BMIm][NTf$_2$] at different dilution factors were similar except for a slight red shift with decreasing dilution factor (Fig. 4a). In contrast to un-irradiated [BMIm][NTf$_2$] solutions that were all colorless, the irradiated [BMIm][NTf$_2$] samples changed from colorless to yellow or orange as dilution factor decreases (Fig. 4b). What color is presented depends on the visible light absorption of each sample. [BMIm][NTf$_2$] at a relatively high dilution factor exhibited an obvious peak at 290 nm and a long tail of absorption band extending beyond 400 nm. However, as the absorbance value at 400 nm was too low (less than 0.1), [BMIm][NTf$_2$] with a high dilution factor was colorless. With increasing concentration of [BMIm][NTf$_2$], the intensity of UV-Vis absorption in a wide range increased. Specifically, at a dilution factor of 0, significant enhancement in the intensity of "long tail" was observed and the tail expanded to 650 nm. The long tail of absorption was also observed for un-irradiated [BMIm][PF$_6$], which was an implication of the existence of various associated species that are energetically different.[34] Accordingly, it is supposed that the "tail" in the UV-Vis spectra of [BMIm][NTf$_2$] after irradiation is ascribable to the associated species which are formed during irradiation. As shown in Fig. S6 (ESI†), though structural heterogeneity and aggregation at the molecular level exist in un-irradiated imidazolium RTILs,[35, 36] un-irradiated [BMIm][NTf$_2$] samples showed almost no visible path of light when a beam of light passes through them. In contrast, obvious Tyndall effect was observed for [BMIm][NTf$_2$] after irradiation. This implies that radiation induces aggregation of [BMIm][NTf$_2$] and larger associated species in the size range from several nanometers to dozens of nanometers are formed during irradiation. These associated species can absorb longer-wavelength light. At higher concentration of irradiated [BMIm][NTf$_2$], the associated species are in a higher density and more portions of longer-wavelength light are absorbed, which explains the enhanced intensity of the "long tail" as well as the color change.

Accordingly, the cause for the color change of [BMIm][NTf$_2$] after irradiation can be explained as follows: during gamma irradiation, "double-bond products" are produced, resulting in a new absorption band centered at 290 nm; at the same time, these radiolysis products associate with other [BMIm][NTf$_2$] molecules that do not undergo radiolysis, yielding various associated structures that absorb light with wavelengths longer than 400 nm and producing a certain color. After HNO$_3$ or O$_3$ treatment, the "double-bond products" are oxidized and the decoloration of irradiated RTILs can be achieved. As a result of the complexity of radiation-induced reactions and radiolytic products, it is probable that there exist other small quantity of colored species in irradiated [BMIm][NTf$_2$] besides the "double-bond products". The study on other kinds of colored species of [BMIm][NTf$_2$] and radiation-induced color change of other kinds of RTILs, such as ammonium RTILs and pyridinium RTILs, is still underway in our laboratory.

Conclusions

This work is concentrated mainly on the radiation-induced color change of [BMIm][NTf$_2$]. No major decomposition occurred in [BMIm][NTf$_2$] and [BMPyrr][NTf$_2$] after γ-irradiation at 400 kGy. Following irradiation at argon atmosphere, all the tested RTILs showed color darkening and enhanced spectral absorption. The enhanced UV absorption is mainly attributed to the radiolysis of organic cations in RTILs. Besides HNO$_3$ oxidation, the decoloration of irradiated RTILs

This journal is © The Royal Society of Chemistry 2014

Phys. Chem. Chem. Phys., 2014, **00**, 1-6 | **5**

can also be achieved by simply purging O_3 into the irradiated RTILs. Based on the experimental and computational results, it is proposed that the degradation products with double bonds in the aliphatic chains of cations (or radiolysis products of [BMIm][NTf$_2$]) account for the enhanced UV absorption of irradiated [BMIm][NTf$_2$] and that the presence of various energetically-different associated structures containing the "double-bond products" is the direct reason for the radiation-induced color change of [BMIm][NTf$_2$]. It is expected that these methods we introduced can also be employed to the study on color change of more RTILs during irradiation.

Acknowledgements

Notes and references

a Beijing National Laboratory for Molecular Sciences, Department of Applied Chemistry, College of Chemistry and Molecular Engineering, Peking University, 100871, Beijing, P. R. China
b Beijing National Laboratory for Molecular Sciences, Institute of Theoretical and Computational Chemistry, State Key Laboratory of Rare Earth Materials Chemistry and Applications, College of Chemistry and Molecular Engineering, and Center for Computational Science and Engineering, Peking University, 100871, Beijing, P. R. China
c Key laboratory of Nuclear Radiation and Nuclear Energy Technology and Key Laboratory for Biomedical Effects of Nanomaterials & Nanosafety, Institute of High Energy Physics, Chinese Academy of Sciences, 100049, Beijing, P. R. China
† Electronic Supplementary Information (ESI) available: ATR-IR and ^{1}H NMR spectra of RTILs prior to and after irradiation; UV–Vis and ^{1}H NMR spectra of RTILs before and after decoloration treatment; evidence to support the formation of "double-bond products" in irradiated [BMPyrr][NTf$_2$]; figure displaying Tyndall effect of [BMIm][NTf$_2$] after irradiation. See DOI: 10.1039/b000000x/

1. T. Welton, *Chem Rev*, 1999, **99**, 2071-2083.
2. K. Binnemans, *Chem. Rev.*, 2007, **107**, 2592-2614.
3. A. E. Visser and R. D. Rogers, *J. Solid State Chem.*, 2003, **171**, 109-113.
4. M. P. Jensen, J. Neuefeind, J. V. Beitz, S. Skanthakumar and L. Soderholm, *J. Am. Chem. Soc.*, 2003, **125**, 15466-15473.
5. S. Dai, Y. H. Ju and C. E. Barnes, *J. Chem. Soc., Dalton Trans.*, 1999, 1201-1202.
6. T. Erdmenger, C. Guerrero-Sanchez, J. Vitz, R. Hoogenboom and U. S. Schubert, *Chem. Soc. Rev.*, 2010, **39**, 3317-3333.
7. R. Michalski, A. Sikora, J. Adamus and A. Marcinek, *J.Phys. Chem. A*, 2010, **114**, 11552-11559.
8. S. M. Chen, Y. D. Liu and G. Z. Wu, *Nanotechnology*, 2005, **16**, 2360-2364.
9. S. J. Wang, Y. W. Zhang, H. L. Ma, Q. L. Zhang, W. G. Xu, J. Peng, J. Q. Li, Z. Z. Yu and M. Zhai, *Carbon*, 2013, **55**, 245-252.
10. D. Allen, G. Baston, A. E. Bradley, T. Gorman, A. Haile, I. Hamblett, J. E. Hatter, M. J. F. Healey, B. Hodgson, R. Lewin, K. V. Lovell, B. Newton, W. R. Pitner, D. W. Rooney, D. Sanders, K. R. Seddon, H. E. Sims and R. C. Thied, *Green Chem.*, 2002, **4**, 152-158.
11. L. Berthon, S. I. Nikitenko, I. Bisel, C. Berthon, M. Faucon, B. Saucerotte, N. Zorz and P. Moisy, *Dalton Trans.*, 2006, 2526-2534.
12. E. Bosse, L. Berthon, N. Zorz, J. Monget, C. Berthon, I. Bisel, S. Legand and P. Moisy, *Dalton Trans.*, 2008, 924-931.
13. I. A. Shkrob, T. W. Marin, S. D. Chemerisov and J. F. Wishart, *J. Phys. Chem. B*, 2011, **115**, 3872-3888.
14. I. A. Shkrob, T. W. Marin, S. D. Chemerisov, J. L. Hatcher and J. F. Wishart, *J. Phys. Chem. B*, 2011, **115**, 3889-3902.
15. I. A. Shkrob, T. W. Marin, S. D. Chemerisov, J. Hatcher and J. F. Wishart, *J. Phys. Chem. B*, 2012, **116**, 9043-9055.
16. I. A. Shkrob, T. W. Marin, H. Luo and S. Dai, *J. Phys. Chem. B*, 2013, **117**, 14372-14384.
17. I. A. Shkrob, T. W. Marin, J. L. Hatcher, A. R. Cook, T. Szreder and J. F. Wishart, *J. Phys. Chem. B*, 2013, **117**, 14385-14399.
18. I. A. Shkrob, T. W. Marin, J. R. Bell, H. Luo and S. Dai, *J. Phys. Chem. B*, 2013, **117**, 14400-14407.
19. L. Y. Yuan, J. Peng, L. Xu, M. L. Zhai, J. Q. Li and G. S. Wei, *Dalton Trans*, 2008, 6358-6360.
20. L. Y. Yuan, J. Peng, L. Xu, M. L. Zhai, J. Q. Li and G. S. Wei, *J. Phys. Chem. B*, 2009, **113**, 8948-8952.
21. M. Y. Qi, G. Z. Wu, S. M. Chen and Y. D. Liu, *Radiat. Res.*, 2007, **167**, 508-514.
22. M. Y. Qi, G. Z. Wu, Q. M. Li and Y. S. Luo, *Radiat. Phys. Chem.*, 2008, **77**, 877-883.
23. L. Y. Yuan, J. Peng, L. Xu, M. L. Zhai, J. Q. Li and G. S. Wei, *Radiat. Phys. Chem.*, 2009, **78**, 1133-1136.
24. P. Nockemann, K. Binnemans and K. Driesen, *Chem. Phys. Lett.*, 2005, **415**, 131-136.
25. M. J. Frisch, G. W. Trucks, H. B. Schlegel, G. E. Scuseria, M. A. Robb, J. R. Cheeseman, G. Scalmani, V. Barone, B. Mennucci, G. A. Petersson, H. Nakatsuji, M. Caricato, X. Li, H. P. Hratchian, A. F. Izmaylov, J. Bloino, G. Zheng, J. L. Sonnenberg, M. Hada, M. Ehara, K. Toyota, R. Fukuda, J. Hasegawa, M. Ishida, T. Nakajima, Y. Honda, O. Kitao, H. Nakai, T. Vreven, J. A. Montgomery, Jr., J. E. Peralta, F. Ogliaro, M. Bearpark, J. J. Heyd, E. Brothers, K. N. Kudin, V. N. Staroverov, R. Kobayashi, J. Normand, K. Raghavachari, A. Rendell, J. C. Burant, S. S. Iyengar, J. Tomasi, M. Cossi, N. Rega, N. J. Millam, M. Klene, J. E. Knox, J. B. Cross, V. Bakken, C. Adamo, J. Jaramillo, R. Gomperts, R. E. Stratmann, O. Yazyev, A. J. Austin, R. Cammi, C. Pomelli, J. W. Ochterski, R. L. Martin, K. Morokuma, V. G. Zakrzewski, G. A. Voth, P. Salvador, J. J. Dannenberg, S. Dapprich, A. D. Daniels, Ö. Farkas, J. B. Foresman, J. V. Ortiz, J. Cioslowski and D. J. Fox, *Gaussian 09 (Revision A.02)*, Gaussian, Inc.: Wallingford CT, 2009.
26. W. Huang, S. M. Chen, Y. S. Liu, H. Y. Fu and G. Z. Wu, *Radiat. Phys. Chem.*, 2011, **80**, 573-577.
27. I. A. Shkrob, T. W. Marin, S. D. Chemerisov and J. F. Wishart, *J. Phys. Chem. B*, 2011, **115**, 10927-10942.
28. C. N. Sherren, C. Mu, M. I. Webb, I. McKenzie, B. M. McCollum, J.-C. Brodovitch, P. W. Percival, T. Storr, K. R. Seddon, J. A. C. Clyburne and C. J. Walsby, *Chem. Sci.*, 2011, **2**, 2173-2177.
29. A. J. Arduengo, R. L. Harlow and M. Kline, *J. Am. Chem. Soc.*, 1991, **113**, 361-363.
30. A. J. Arduengo, H. V. R. Dias, R. L. Harlow and M. Kline, *J. Am. Chem. Soc*, 1992, **114**, 5530-5534.
31. A. J. Arduengo, F. Davidson, H. V. R. Dias, J. R. Goerlich, D. Khasnis, W. J. Marshall and T. K. Prakasha, *J. Am. Chem. Soc.*, 1997, **119**, 12742-12749.

6 | *Phys. Chem. Chem. Phys.*, 2014, **00**, 1-6

This journal is © The Royal Society of Chemistry 2014

32. I. A. Shkrob, S. D. Chemerisov and J. F. Wishart, *J. Phys. Chem. B*, 2007, **111**, 11786-11793.

33. G. Le Rouzo, C. Lamouroux, V. Dauvois, A. Dannoux, S. Legand, D. Durand, P. Moisy and G. Moutiers, *Dalton Trans.*, 2009, 6175-6184.

34. A. Paul, P. K. Mandal and A. Samanta, *Chem. Phys. Lett.*, 2005, **402**, 375-379.

35. J. N. A. Canongia Lopes and A. A. H. Pádua, *J. Phys. Chem. B*, 2006, **110**, 3330-3335.

36. S. M. Chen, S. J. Zhang, X. M. Liu, J. Q. Wang, J. J. Wang, K. Dong, J. Sun and B. H. Xu, *Phys. Chem. Chem. Phys.*, 2014, **16**, 5893-5906.

Physical Chemistry Chemical Physics Accepted Manuscript

This journal is © The Royal Society of Chemistry 2014

Phys. Chem. Chem. Phys., 2014, **00**, 1-6 | **7**